Dielectric properties of carbon-, silicon-, and germanium-based polymers: A first-principles study

C. C. Wang, G. Pilania, and R. Ramprasad[*]

Department of Chemical, Materials, and Biomolecular Engineering, Institute of Materials Science, University of Connecticut,
97 North Eagleville Road, Storrs, Connecticut 06269, USA

A knowledge of factors that control the electronic structure and dielectric constant of materials would be valuable in the design of new insulators with attractive dielectric properties. In an attempt to systematically and directly understand the role of chemical composition and atomic configuration in determining such properties, we have studied (using first-principles computations) nine homopolymer systems based on XY_2 building blocks, where $X = $ C, Si, or Ge and $Y = $ H, F, or Cl. Two possible generic configurations were explored, and our computations utilized dispersion-corrected semilocal exchange-correlation functionals as well as hybrid functionals. Correlations between stability, electronic structure features, infrared intensities, and the dielectric response are established across the chemical and configurational space considered. Homopolymers containing GeF_2 or $GeCl_2$ building blocks are identified as particularly promising. These systems display large dielectric constant values (regardless of the underlying crystal structure) and may display a large band gap for particular configurations. The design of a polymer insulator with optimal dielectric constant *and* band gap may require consideration of heteropolymers (e.g., involving CH_2 and GeF_2 building blocks). We provide a convenient strategy for the rapid exploration of that extended chemical and configurational space.

PACS number(s): 77.22.−d

I. INTRODUCTION

High-energy-density capacitors are required for several pulsed power and energy storage applications, including food preservation, nuclear test simulations, electric propulsion of ships, and hybrid electric vehicles.[1] The maximum possible stored energy density of a capacitor is given by $U = 0.5\epsilon_0\epsilon E_b^2$, where ϵ_0, ϵ, and E_b are, respectively, the permittivity of free space, the dielectric constant, and the dielectric breakdown field. The current standard dielectric material for high-energy-density capacitor applications is biaxially oriented polypropylene (BOPP),[2] which has a remarkably high electrical breakdown strength (>700 MV/m) but a small dielectric constant ($\sim$2.2). Attempts to surpass the properties of BOPP—including the usage of poly(vinylidene fluoride) based copolymers,[3–6] multilayer films of differing polymers,[7] and polymer nanocomposites[8,9]—have met with limited success, partly due to a lack of sufficient understanding of the fundamental chemical, configurational, and morphological factors that control or limit ϵ and E_b.

In the present work, we consider a restricted class of aliphatic polymers and attempt to identify dominant chemical and atomic-level configurational factors that affect their electronic structure and dielectric properties. We start with polyethylene (PE), which is chemically similar to polypropylene, and subject it to systematic chemical modifications. Homopolymers with a XY_2 repeat unit are considered, with $X = $ C, Si, or Ge and $Y = $ H, F, or Cl. Crystalline PE corresponds to the homopolymer with a CH_2 repeat unit. The motivation for this study is provided by our recent work, which has shown that both the electronic and ionic dielectric constant of PE can be increased by up to a factor of 2 by progressively replacing C atoms with Si atoms in the PE backbone.[10]

A proper assessment of the impact of chemical modifications should also include consideration of the role played by configurational and crystallographic factors. Out of the nine XY_2 homopolymers considered here (henceforth referred

to as just XY_2), crystallographic information is available for CH_2, CF_2, $SiCl_2$, and GeF_2. CH_2, CF_2, and $SiCl_2$ crystallize in an orthorhombic structure, with chains composed of sp^3 hybridized C (or Si) backbones, as shown in Fig. 1(a).[11–14] We refer to this atomic arrangement as the type A structure. The equilibrium structure of the GeF_2 system, although also orthorhombic, is different.[15,16] This is composed of -Ge-F- chains, with the F atoms bridging successive Ge atoms, as shown in Fig. 1(b). Each Ge atom is also bound to an additional terminal F atom. This configuration, henceforth referred to as the type B structure, leads to a lone pair of electrons at each Ge center [in contrast to the sp^3 hybridized C (or Si) atoms in the type A structure]. Both the type A and type B primitive unit cells contain two chains and two XY_2 formula units per chain.

All nine XY_2 homopolymers were considered in both the type A and type B structures in the present study. We find that the type A structure is the only stable one for systems containing C or H. SiF_2 and $SiCl_2$ are stable in the type A structure and metastable in the type B structure, while GeF_2 and $GeCl_2$ display the opposite trend.

Although we assess the stability of the nine XY_2 homopolymers in the two possible structures, our primary interest is their electronic and ionic dielectric constant tensor and the band gap (as a larger band gap generally correlates to a larger intrinsic breakdown field[17]). Not surprisingly, the electronic structures (and band gap) of the type A and type B structures are markedly different from each other. While the four systems which can occur in the latter structure display moderately large band gaps in the 3.6–5.3 eV range, those in the former structure display band gaps that progressively and systematically decrease as the backbone atoms (i.e., X) vary from C to Si to Ge or when the terminal atoms (i.e., Y) vary from H to F to Cl. The electronic part of the dielectric constant in general correlates inversely with the band-gap value, while the ionic contribution is negligible for the C containing systems and large for the Si
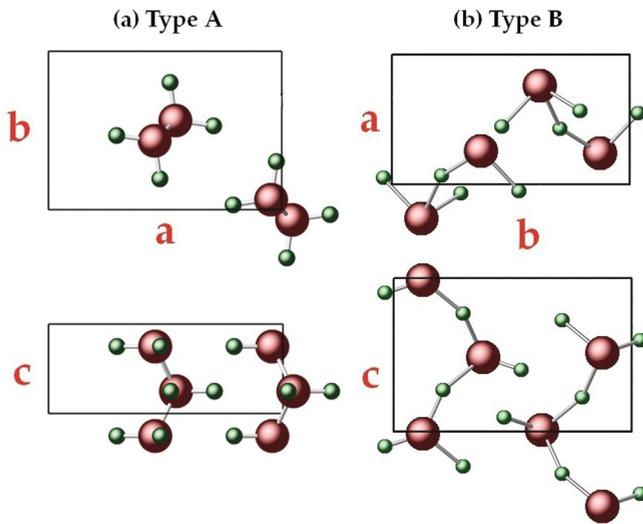
FIG. 1. (Color online) Orthorhombic unit cells of the XY_2 homopolymers in the (a) type A and (b) type B structures, with a, b, and c representing the three lattice parameters. Red and green spheres represent the X and Y atoms, respectively.

and Ge containing systems. These findings are captured in the plot shown in Fig. 2.

The above trends indicate the need for optimization of properties through construction of heteropolymers. Since the possibilities for such heteropolymers are, in principle, infinite, a rapid method to estimate the dielectric constant and band gap would be beneficial. As a step in that direction, we present an efficient scheme for the computation of the dielectric constant of bulk heteropolymers based on individual chain computations. The results of the single-chain based method are further validated against the crystal structure based calculations for all the polymers studied here.
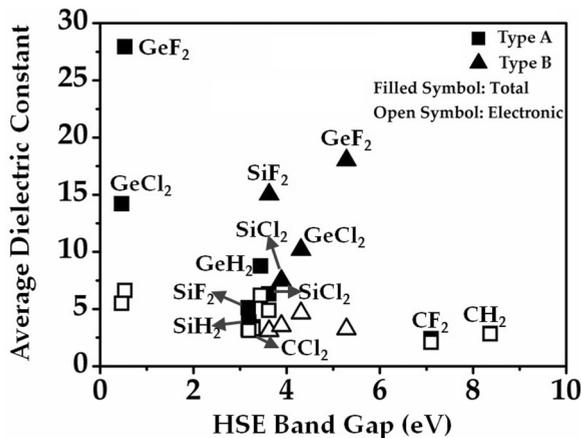

FIG. 2. The average dielectric constant vs the band gap of XY_2 polymers in the type A and type B structures. Filled and open symbols represent total (electronic plus ionic) and electronic contributions to the dielectric constant, respectively. The band gap was computed using the Heyd-Scuseria-Ernzerhof (HSE) hybrid exchange-correlation functional. For clarity, system labels are placed next to the filled symbols alone. The open symbol corresponding to a labeled filled symbol is directly below at the same value of the band gap.

The rest of the paper is organized as follows. In Sec. II, we provide details concerning the first-principles computational methodology used. In Sec. III, we present results of the structural properties and stability of the nine homopolymers in the two possible crystal structures, before moving onto a detailed discussion of their electronic and dielectric properties. The strategy for the rapid estimation of the dielectric constant of polymers, and the validation of this strategy, are also presented in this section. Finally, our conclusions are summarized in Sec. IV.

II. METHODOLOGY

Density functional theory (DFT), as implemented in the Vienna *ab initio* simulation package (VASP),[18] was used to determine the structural and electronic properties of the nine XY_2 polymers in the two possible crystal structures. The Perdew, Burke, and Ernzerhof (PBE) functional[19] augmented with the Grimme D2 van der Waals correction (PBE-D2),[20,21] projector-augmented wave frozen-core potentials,[22,23] and a cutoff energy of 500 eV for the plane-wave expansion of the wave functions were used. The choice of the PBE-D2 functional was motivated by our recent study.[24] Conventional local density approximation and generalized gradient approximation (e.g., PBE) functionals lead to significant underestimation and overestimation, respectively, of the polymer crystal volumes owing to improper treatment of the interchain van der Waals interactions; although the PBE-D2 functional does not completely eliminate this shortcoming, it mitigates this deficiency to a large extent (polymer crystal volumes are still underestimated by the PBE-D2 functional by about 7% on average).[24]

Geometries optimized using the PBE-D2 functional were then used to determine the dielectric constant tensor using density functional perturbation theory (DFPT).[25] DFPT has been widely used in studies of the vibrational, dielectric, and optical properties of a variety of materials, including elemental and compound semiconductors,[26,27] simple and complex oxides,[28,29] and polymers.[30] As the PBE functional is known to underestimate band gaps of insulators, the Heyd-Scuseria-Ernzerhof HSE06 functional[31] (with the mixing and inverse screening parameters set to 0.25 and 0.207 Å^{-1}, respectively) was used to obtain corrected band-gap values.

III. RESULTS AND DISCUSSION

A. Stability and structure of XY_2 polymers

Systems containing C or H could be stabilized only in the type A structure. Geometry optimizations of these systems starting with the type B structure always converge to the type A structure. Although the other four systems, namely, SiF_2, GeF_2, $SiCl_2$, and $GeCl_2$, could be stabilized in both the type A and type B structures, SiF_2 and $SiCl_2$ are more stable in the type A structure, while the type B structure is the more favored one for GeF_2 and $GeCl_2$. The relative energy (ΔE, per XY_2 unit) for the four polymers that could be stabilized in the type B structure, measured with respect to the total energy in the corresponding type A structure, is reported in Table I. These findings are consistent with the expectations that C (Ge) displays the most (least) resistance to house a lone pair and

TABLE I. Calculated equilibrium lattice constants and cohesive energy [as defined in Eq. (1)] for the XY_2 polymers in the type A and type B structures. The values in parentheses are from experiments (see text for references). For the four polymers stable in the type B structure, the relative energy (ΔE, per XY_2 unit), measured with respect to the total energy in the corresponding type A structure, is also reported.

Type A	a (Å)	b (Å)	c (Å)	$E_{\rm coh}$ (eV)	
CH_2	6.67 (7.12)	4.54 (4.85)	2.55 (2.55)	0.11 (0.1)	
SiH_2	8.02	4.38	3.94	0.14	
GeH_2	7.62	4.33	4.12	0.25	
CF_2	8.42 (8.73)	5.91 (5.69)	2.65 (2.62)	0.10	
SiF_2	9.27	4.81	4.17	0.20	
GeF_2	8.87	3.95	4.61	0.56	
CCl_2	10.49	7.24	2.96	0.22	
$SiCl_2$	11.14 (13.35)	7.96 (6.78)	4.10 (4.06)	0.23	
$GeCl_2$	11.37	7.34	4.98	0.09	
Type B	a (Å)	b (Å)	c (Å)	$E_{\rm coh}$ (eV)	ΔE (eV)
SiF_2	4.49	9.00	4.82	0.15	0.87
GeF_2	4.39 (4.68)	8.01 (8.31)	5.19 (5.18)	0.38	−0.50
$SiCl_2$	9.16	7.71	4.82	0.26	1.06
$GeCl_2$	9.74	7.82	4.27	–	−0.35

H displays no tendency to be a bridging element. Subsequent results are reported for all nine XY_2 polymers in the type A structure and only four polymers (SiF_2, $SiCl_2$, GeF_2, and $GeCl_2$) in the type B structure.

The optimized lattice parameters, calculated for all the stable XY_2 polymers, are also reported in Table I, with the available experimental values provided in parentheses.[13–15,32] For the XY_2 polymers in the type A structure, the lattice parameters normal to the polymer chains (i.e., a and b) are determined by the weak interchain van der Waals interactions, while the lattice parameter along the polymer chain axis (i.e., c) depends on the intrachain covalent C-C, Si-Si, or Ge-Ge interactions. We thus expect c to depend on the covalent radius of the backbone element. Our results for c indeed show a systematic increase going from CY_2 to SiY_2 to GeY_2, while a and b do not show any particular trend. Type B structures, owing to the lone pair of electrons and the terminal halogens, display interchain interactions that couple the three lattice parameters, and hence the trends described above are not entirely borne out for these systems.

Table I also lists the cohesive energy, $E_{\rm coh}$, representing the energy required to separate the polymer crystal to individual chains. $E_{\rm coh}$ (per XY_2 formula unit) is defined as

$$E_{\rm coh} = \frac{2E_{\rm chain} - E_{\rm crystal}}{4},\qquad(1)$$

where $E_{\rm chain}$ is the total energy of an isolated polymer chain and $E_{\rm crystal}$ is the total energy of the polymer crystal. The factors 2 and 4 account, respectively, for the fact that there are two chains and four XY_2 formula units per unit cell. The calculated cohesive energy of polyethylene (CH_2), 0.11 eV, agrees well with the corresponding experimental value of 0.1 eV.[33] We find that in both type A and type B structures, GeF_2 has the highest cohesive energy, indicating strong interchain interactions. No $E_{\rm coh}$ result is shown for $GeCl_2$ in the type B structure because a single-chain configuration is not stable in this case.

B. Electronic properties of XY_2 polymers

Table II presents the band gaps of all XY_2 polymers both in type A and type B structures. Past DFT studies of the electronic structure of CH_2 have utilized (semi)local functionals,[34] which predict band-gap values of 5.7 eV (within the generalized gradient approximation) and 6.0 eV (within the local-density approximation), underestimated with respect to the experimental value of 8.8 eV.[35] HSE06 is used in our work, which, as can be seen from Table II, provides band-gap predictions for CH_2 and CF_2, in close agreement with the corresponding experimental estimates.[35,36] Considering the type A systems first, we see that CH_2 displays the largest band gap (8.4 eV), which progressively and systematically decreases as the backbone atom is varied from C to Si to Ge or when the terminal atom is varied from H to F to Cl. GeF_2 and $GeCl_2$ in the type A structure display the smallest band gaps (of about 0.5 eV). These band-gap trends may be understood in terms of enhanced σ conjugation as one moves from C to Si to Ge backbones. On the other hand, GeF_2, $GeCl_2$, SiF_2, and $SiCl_2$, when in the type B structure, display much larger band gaps (compared to the same systems in the type A structure) of 3.6–5.3 eV.

The dramatic variation in the band gap with structure may be understood better by inspection of the electronic density of states (DOS) and atom projected DOS plots shown in Fig. 3. XH_2 systems display large covalent bonding between X and H, as characterized by the appearance of both X- and H-derived DOS in both the valence- and conduction-band manifolds. CF_2 and CCl_2 display more ionicity, as indicated by the strong F or Cl (C) character of the valence (conduction) band. The DOS of GeF_2 and $GeCl_2$ (and to some extent, SiF_2 and $SiCl_2$), when in the type A structure, are particularly striking in that the small band gap of these systems is a consequence of defectlike states and peaks in the neighborhood of the valence band maximum and conduction band minimum. These features are indicative of the poor stability of such systems when in the type A structure. Indeed, these systems in the type B structure are particularly stable (especially GeF_2 and $GeCl_2$), with a larger

TABLE II. Calculated band gap and dielectric constant for the XY_2 polymers in the type A and type B structures. The values in parenthesis are the experimental band-gap values for CH_2[35] and CF_2.[36] ϵ_{xx}^{elec}, ϵ_{yy}^{elec}, and ϵ_{zz}^{elec} represent the diagonal components of the electronic dielectric constant tensor, while ϵ_{xx}^{tot}, ϵ_{yy}^{tot}, and ϵ_{zz}^{tot} are the diagonal elements of the total dielectric constant tensor (i.e., including electronic and ionic contributions). The polymers are oriented such that the chain axis is parallel to the z direction.

Type A	Band gap (eV)	ϵ_{xx}^{elec}	ϵ_{yy}^{elec}	ϵ_{zz}^{elec}	ϵ_{xx}^{tot}	ϵ_{yy}^{tot}	ϵ_{zz}^{tot}
CH_2	8.37 (8.80)	2.74	2.83	2.92	2.78	2.88	2.92
SiH_2	3.62	4.01	4.13	6.48	4.69	4.92	9.34
GeH_2	3.44	4.96	5.18	8.45	6.07	5.93	14.26
CF_2	7.1 (7.66)	2.03	2.04	2.17	2.33	2.33	2.51
SiF_2	3.18	2.25	2.27	5.19	3.18	3.47	8.64
GeF_2	0.53	3.05	5.27	11.54	4.71	26.95	52.13
CCl_2	3.28	3.17	3.31	3.31	3.35	3.56	3.42
$SiCl_2$	3.19	2.74	2.78	3.85	3.14	3.19	5.25
$GeCl_2$	0.46	3.05	3.07	10.35	3.73	4.65	34.25
Type B	Band gap (eV)	ϵ_{xx}^{elec}	ϵ_{yy}^{elec}	ϵ_{zz}^{elec}	ϵ_{xx}^{tot}	ϵ_{yy}^{tot}	ϵ_{zz}^{tot}
SiF_2	3.62	2.98	2.73	3.57	7.49	5.12	32.49
GeF_2	5.28	3.12	3.26	3.37	11.52	21.49	21.05
$SiCl_2$	3.89	3.65	3.33	3.63	7.05	5.33	10.10
$GeCl_2$	4.31	5.28	4.31	4.34	11.09	6.32	13.16

band gap and "clean" DOS in the neighborhood of the band edges (cf. Fig. 3).

C. Dielectric properties of XY_2 polymers

The electronic and total (electronic plus ionic) dielectric constant tensors were calculated using DFPT. The diagonal components of the tensor along the three principal axes of the nine XY_2 polymers in the type A structure and the four stable systems in the type B structure are presented in Table II and Fig. 4. Let us consider the case of CH_2, which is the only case for which experimental dielectric constant results are

available. In this system, while the ionic contribution to the dielectric constant is negligible, the electronic contribution averaged along the three principal axes is computed to be around 2.8. This value is somewhat higher than the reported average experimental value of about 2.2 for polyethylene.[37] This discrepancy may be explained by considering two factors. First, the experimental value is for *semicrystalline* polyethylene, containing a fair amount of amorphous regions of lower density than crystalline polyethylene, which, consequently, will display a smaller value of the dielectric constant than crystalline polyethylene. Second, considering that the PBE-D2 functional used here tends to underestimate the volume of
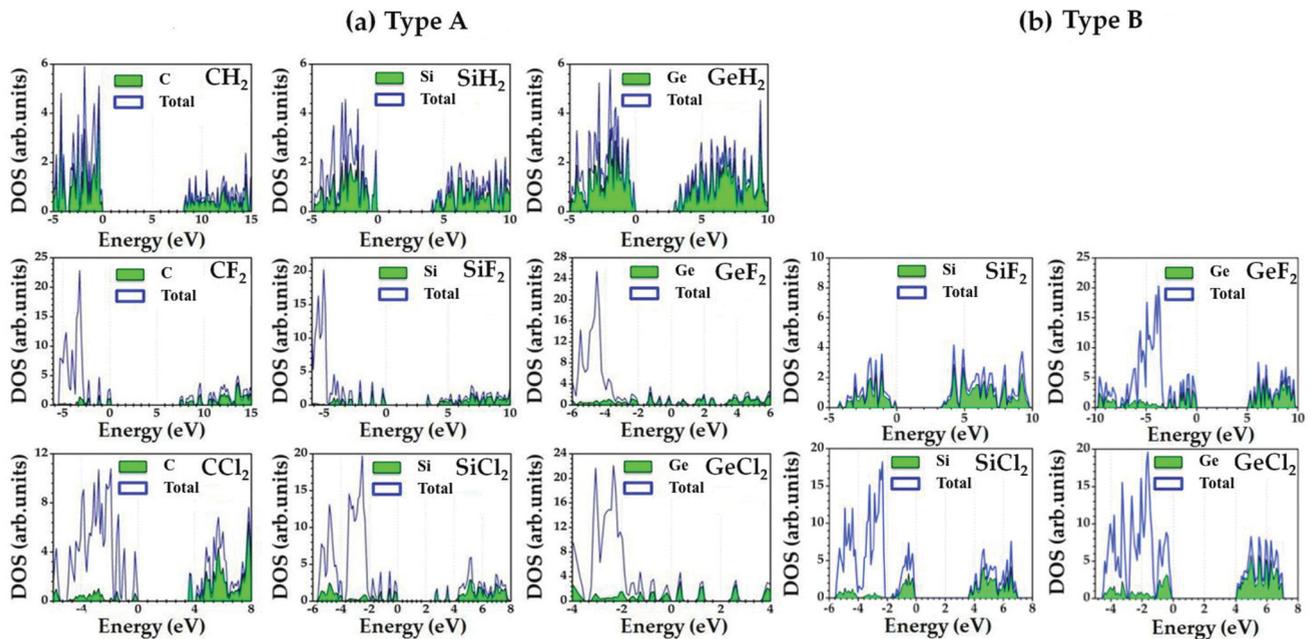

FIG. 3. (Color online) Density of states and site projected density of states (projected onto each of the constituent elements in the polymer) of XY_2 polymers in (a) type A and (b) type B structures.
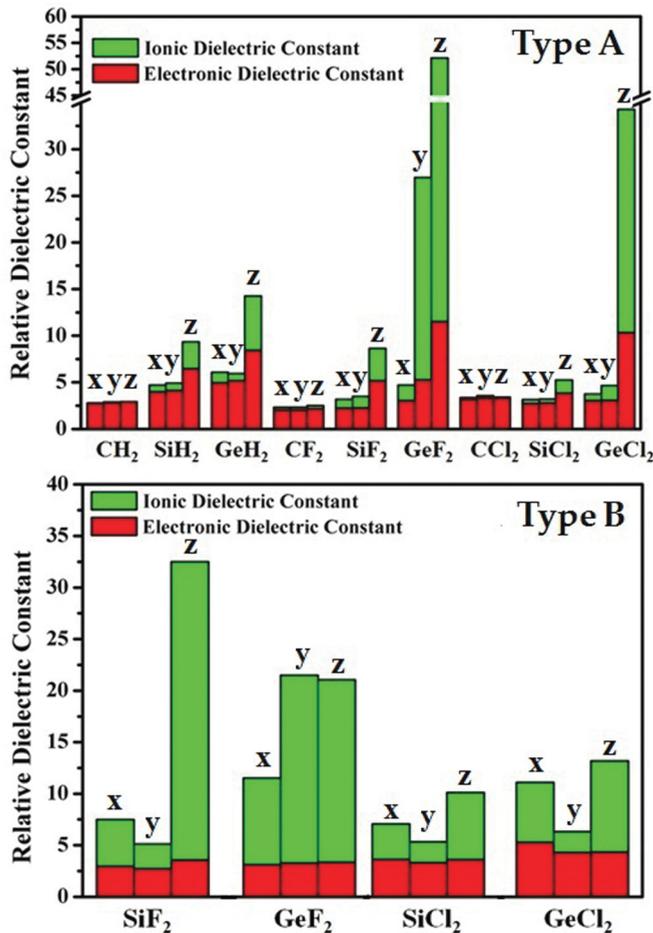
FIG. 4. (Color online) Diagonal components of the dielectric constant tensors of XY_2 polymers in type A (top) and type B (bottom) structures. Red and green filled areas represent the electronic and ionic contributions, respectively.

(indeed, the electronic contribution to the polarizability may be written in terms of a sum over electronic transitions from the valence band to the conduction band manifolds[38]). Figure 2, for instance, shows an approximate inverse relationship between the electronic part of the dielectric constant and the band gap for both type A and type B structures.

The ionic contribution to the dielectric constant (total minus electronic), on the other hand, is not directly correlated with the band gap [especially when type A and type B structures are considered together (see Fig. 2)], as this contribution is purely controlled by the infrared (IR) active zone center phonon modes (i.e., the modes that display a time-varying dipole moment).[39,40] The extent to which each IR-active phonon mode contributes to the dielectric tensor is determined by the frequency of the mode (the smaller the frequency, the larger the dielectric constant) and the IR intensity (I_i^{IR}) of the corresponding zone center mode (the larger the IR intensity, the larger the dielectric constant), which is given by[41,42]

$$I_i^{\mathrm{IR}} \propto \sum_\alpha \left| \sum_{k,\beta} Z^*_{k,\alpha\beta} X_i(k,\beta) \right|^2,$$

where i labels the modes, k labels atoms, and α and β are the Cartesian coordinates. $Z^*_{k,\alpha\beta}$ and $X_i(k,\beta)$ represent appropriate components of the Born effective charge tensor and the phonon mode eigenvector, respectively. For IR-inactive phonon modes, this intensity vanishes. Figure 5 shows the dominant IR-active modes at the corresponding frequencies for all the stable polymers in the type A and type B structures. The increase of the ionic contribution to the dielectric constant as one goes from CY_2 to SiY_2 to GeY_2 can be clearly seen to be due to the increase in the IR intensities of the dominant IR-active modes and the decrease of the frequencies of the corresponding modes. We also note that the dominant IR-active modes are the X-Y stretch and the Y-X-Y wagging modes. In the case of the type B structures, again the large ionic contribution arises because of low-frequency IR-active stretching and wagging modes. Furthermore, we also note that none of the systems we consider [i.e., the nine type A and the four type B structures (cf. Fig. 5)] display zone center phonon modes with imaginary frequency. This indicates that the structures considered correspond to local minima in energy within the constraints of the unit cell volumes chosen here.

Figure 2, which collects the dielectric constant and band-gap results for all XY_2 homopolymers considered, clearly shows the benefit of introducing Ge in the backbone of polymers (in either the type A or type B structures). While Ge containing homopolymers in the type A structure may also simultaneously lead to undesirable small band-gap values, heteropolymers containing GeY_2 and units such as CH_2 may offer tradeoffs between the dielectric constant and band-gap values (we note that one of our main goals is to identify polymer systems with large dielectric constants and, simultaneously, large band-gap values).

D. Alternate convenient method to compute dielectric constant

The above results are indicative of the importance of studying heteropolymers containing GeY_2 units. The investigation of the myriad of such heteropolymer possibilities

polymer crystals (by about 7% on average[24]), the dielectric constant calculated at the geometry determined using the PBE-D2 functional is expected to be higher than it should be by about that same amount. Specifically, in the case of CH_2, the volume determined using the PBE-D2 functional is lower than the experimental result by around 12% (cf. Table I). Thus, our dielectric constant result of 2.8 can be taken to be about 12% higher than the true value. The above two factors thus bridge the gap between the computed dielectric constant value of 2.8 and the measured value of 2.2.

We next survey the general trends across the chemical series we have considered. In general, as X in XY_2 varies from C to Si to Ge, both the electronic and ionic contributions to the dielectric constant increase systematically. While substitution of H with F or Cl only slightly modulates the electronic part of the dielectric constant, the most striking observation is perhaps the large value of the ionic contribution to the dielectric constant when Ge is present in the backbone. In the case of the type B structure, both the SiF_2 and the GeF_2 systems show relatively high dielectric constant values.

The behavior of the electronic contribution to the dielectric constant may be understood in terms of the electronic structures for systems in both the type A and type B structures
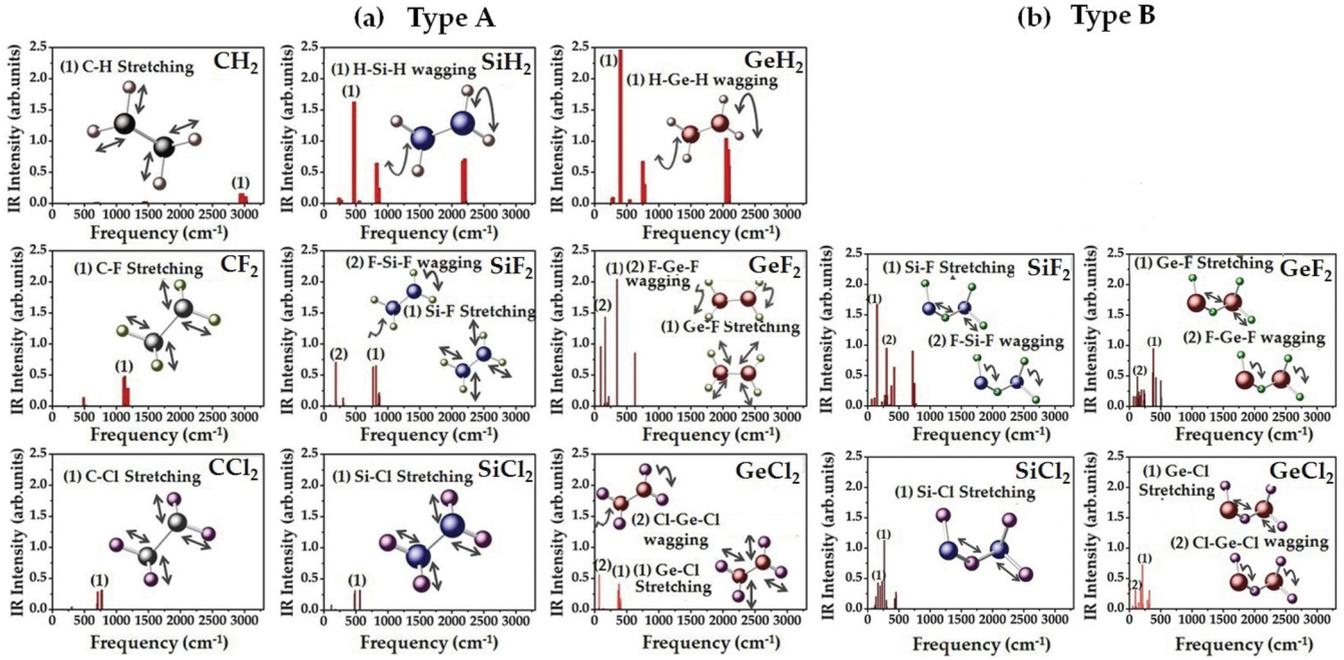
FIG. 5. (Color online) IR intensity of the IR-active zone center phonon modes of XY_2 polymers in (a) type A and (b) type B structures. The characters of the dominant IR-active modes are illustrated in the figure.

is confounded by the necessity of a knowledge of the appropriate crystal structure to be used in such computations (which, in general, may not be available). Moreover, even if such information is available (or can be "guessed"), each computation may be time consuming. In order to reduce the time involved in each such computation, and to obtain rapid estimates of the dielectric constant and band-gap values in the absence of reliable crystallographic information, we have developed a method that is based on purely single-chain computations. On average, this method is approximately 2.5 times faster than the crystal based method presented above. We note that strategies to capture the dielectric response of larger

(or infinite) systems through extrapolation from calculations involving smaller units have been attempted in the past,[43,44] but such efforts are still in a state of infancy.

As shown in Fig. 6(a), we consider an isolated infinite chain of a polymer placed in a supercell volume V_{tot} and use DFPT to compute its dielectric constant. We note that the dielectric constant calculated from DFPT for such a supercell includes the contributions from the polymer as well as from the vacuum region of the supercell. Treating the supercell as a vacuum-polymer composite, effective medium theory may then be used to estimate the dielectric constant of the polymer alone, following recent work.[29]
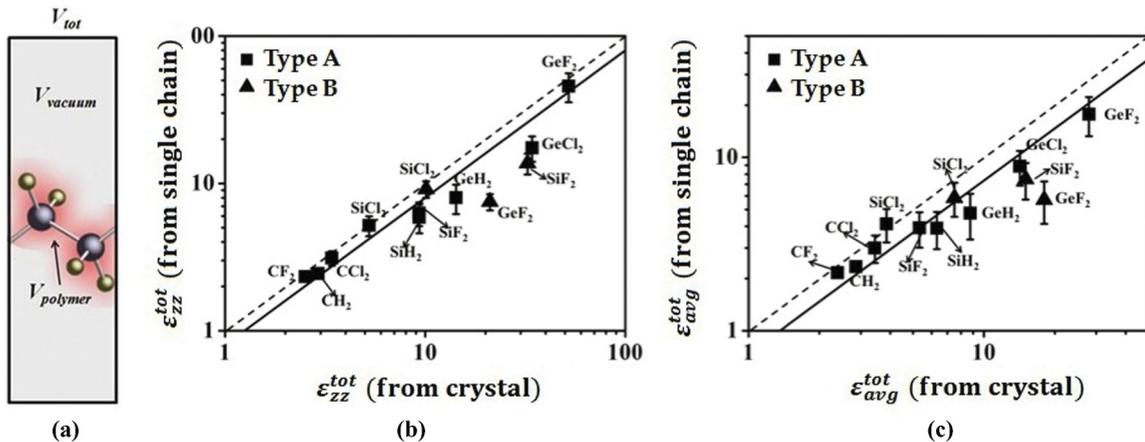

FIG. 6. (Color online) (a) Single-chain model represented as a polymer-vacuum composite. Comparison of the single-chain based results vs the full crystal results for (b) the total dielectric constant along the chain direction and (c) the orientational-averaged dielectric constant. Best fits of the single-chain vs crystal results of type A systems are shown as solid lines. The discrepancy between the two schemes is given by the displacement between the solid and dashed lines.

According to the Maxwell-Garnett equation, the principal components of the dielectric constant of a vacuum-filler composite ϵ_{ii} containing a volume fraction δ of polarizable fillers (a polymer chain in this case) with dielectric constant $\epsilon_{ii}^{\text{polymer}}$ can be written as[45]

$$\frac{\epsilon_{ii} - 1}{1 + (\epsilon_{ii} - 1)P_i} = \delta \frac{\epsilon_{ii}^{\text{polymer}} - 1}{1 + \left(\epsilon_{ii}^{\text{polymer}} - 1\right)P_i}. \quad (2)$$

Here, i represents the Cartesian axes x, y, or z, and P_i is a geometry-dependent depolarizing factor.[46–48] In our case, assuming that the polymer chain is along the z direction, $P_z = 0$, and $P_x = P_y = 0.5$. This leads to the following formula for the axial and off-axis components of the dielectric constant:[49,50]

$$\epsilon_{zz} - 1 = \delta\left(\epsilon_{zz}^{\text{polymer}} - 1\right), \quad (3)$$

$$\frac{\epsilon_{xx} - 1}{\epsilon_{xx} + 1} = \delta \frac{\epsilon_{xx}^{\text{polymer}} - 1}{\epsilon_{xx}^{\text{polymer}} + 1}. \quad (4)$$

In these equations, δ ($= V_{\text{polymer}}/V_{\text{tot}}$) is the volume fraction of the polymer in the supercell, as shown in Fig. 6. In order to use this method to estimate the dielectric constant of the polymer alone, i.e., $\epsilon_{ii}^{\text{polymer}}$, the volume occupied by the polymer chain in the supercell is needed. Here, a procedure based on charge-density cutoffs is used to estimate the volume. If the electronic charge density is larger than a cutoff value at a particular location, then this location is deemed occupied by the polymer. In order to determine the charge-density cutoff value, we have considered several polymers that have experimental volumes (or densities) available to determine the charge-density cutoff value that would result in the experimental density. The polymers used for this analysis include polyethylene, polypropylene, polyacetylene, polythiophene, polypyrole, polydimethylsiloxane, etc. In general, we find that the charge-density cutoff needs to be in the 0.003 to 0.007 electron/Å^3 range in order to reproduce the experimental densities. We note that this range of charge-density cutoffs translates to a range of volumes V_{polymer} and hence to error bars in the calculated dielectric constants using Eqs. (3) and (4).

To validate the single-chain based method, we compare the results of this method with those from the three-dimensional crystal based calculations presented in Sec. III C. Figures 6(b) and 6(c) show a comparison between the total dielectric constants along the chain direction ($\epsilon_{zz}^{\text{tot}}$) and the orientationally averaged total dielectric constant ($\epsilon_{\text{avg}}^{\text{tot}}$), respectively, obtained using the two methods. In general, the single-chain method underestimates the dielectric constant relative to the crystal based method by about 20% (for $\epsilon_{zz}^{\text{tot}}$) and about 30% (for $\epsilon_{\text{avg}}^{\text{tot}}$), as shown by the best-fit lines in Figs. 6(b) and 6(c). The discrepancy between the two methods can be attributed to two factors. First, the PBE-D2 functional used in our study tends to underestimate the volume of the polymer crystals by about 7% on average (but by about 12% for the specific case of CH_2), which results in the overestimation of the dielectric constant computed using the crystal approach (note that the chain approach does not suffer from this inadequacy, as the appropriate van der Waals volume occupied by a chain was determined using a charge-density cutoff criterion which

was fitted to experimental density results for a benchmark set of polymers). Second, interchain interactions are completely neglected in the single-chain computations. The interchain interactions tend to "soften" the intrachain phonon modes and, consequently, increase the dielectric constant values. This factor is especially true in two situations or cases: (1) the type B structures display lone pair electrons, and hence these systems display the maximum discrepancy between the single-chain and crystal based results, as can be seen from Fig. 6; and (2) the off-axis components of the dielectric tensor are most affected by the interchain interactions, and hence $\epsilon_{\text{avg}}^{\text{tot}}$ predictions of the single-chain approach display a larger discrepancy than $\epsilon_{zz}^{\text{tot}}$ with the crystal results.

The above observations indicate that the single-chain approach is most reliable for the computation of $\epsilon_{zz}^{\text{tot}}$ for type A structures and less reliable for all other cases. Nevertheless, the correct trends are indeed captured by the single-chain based approach, and hence we believe that this scheme will be valuable in situations when crystal structure information of specific polymers is not available (e.g., when it is not clear how the chains will organize with respect to each other).

IV. SUMMARY

The intent of this investigation was to identify dominant chemical and configurational factors that control the electronic structure and dielectric response of a restricted class of aliphatic polymers. The chemical space was explored by considering nine homopolymers based on XY_2 building blocks, where $X = $ C, Si, or Ge and $Y = $ H, F, or Cl. Two different prototypical configurations were considered for each of these polymers, one in which the polymer backbone is purely composed of X atoms (referred to as the type A structure) and the second one composed of -X-Y- chains in the backbone, i.e., with a Y atom bridging adjacent X atoms (referred to as the type B structure). The identified correlations between stability, electronic structure, and dielectric response (and our future outlook) may be summarized as follows.

The type A structure is the only stable one for systems containing C or H. The SiF_2 and $SiCl_2$ homopolymers are stable in the type A structure and metastable in the type B structure, while GeF_2 and $GeCl_2$ display the opposite trend.

XY_2 homopolymers in the type A structure display band gaps and dielectric constants that systematically change as the backbone atoms (i.e., X) vary from C to Si to Ge or when the terminal atoms (i.e., Y) vary from H to F to Cl.

The electronic part of the dielectric constant, in general, correlates inversely with the band-gap value, while the ionic part of the dielectric constant is largely controlled by IR-active X-Y stretch and Y-X-Y wagging phonon modes.

Systems containing Ge are identified as particularly promising for applications requiring insulators with a high dielectric constant. For example, GeF_2 in the type A structure displays a large orientationally averaged dielectric constant value of 28 (compared to the 2.8 value of CH_2), but it has a small band-gap value of about 0.5 eV (the corresponding value for CH_2 is 8.4 eV). SiF_2, $SiCl_2$, GeF_2, and $GeCl_2$ in the type B structure simultaneously display moderately large band-gap (3.6–5.3 eV) and dielectric constant (8–18) values.

It may be desirable to consider heteropolymers composed of GeF_2 and CH_2 units to simultaneously optimize the dielectric constant and the band-gap value. In order to aid in an efficient search of the chemical space spanned by such heteropolymers, a convenient strategy for the computation of the dielectric constant of bulk polymers using single-chain computations is presented.

*rampi@ims.uconn.edu

[1] P. F. Flynn, *Meeting the Energy Needs of Future Warriors* (National Academics, Washington, D.C., 2004).

[2] E. J. Barshaw, J. White, M. J. Chait, J. B. Cornette, J. Bustamante, F. Folli, D. Biltchick, G. Borelli, G. Picci, and M. Rabuffi, IEEE Trans. Magn. **43**, 223 (2007).

[3] V. Ranjan, M. Buongiorno-Nardelli, and J. Bernholc, Phys. Rev. Lett. **108**, 087802 (2012).

[4] V. Ranjan, L. Yu, M. Buongiorno-Nardelli, and J. Bernholc, Phys. Rev. Lett. **99**, 047801 (2007).

[5] B. Chu, X. Zhou, K. L. Ren, B. Neese, M. Lin, Q. Wang, F. Bauer, and Q. M. Zhang, Science **313**, 334 (2006).

[6] F. Guan, J. Pan, J. Wang, Q. Wang, and L. Zhu, Macromolecules **43**, 384 (2010).

[7] M. A. Wolak, M.-J. Pan, A. Wan, J. S. Shirk, M. Mackey, A. Hiltner, E. Baer, and L. Flandin, Appl. Phys. Lett. **92**, 113301 (2008).

[8] A. L. An, S. A. Boggs, and J. P. Calame, *Proceedings of the 2006 IEEE International Symposium on Electrical Insulation* (IEEE, New York, 2006), pp. 466–469.

[9] V. Tomer and C. A. Randall, J. Appl. Phys. **104**, 074106 (2008).

[10] C. C. Wang and R. Ramprasad, J. Mater. Sci. **46**, 90 (2011).

[11] G. Avitabile, R. Napolitano, B. Pirozzi, K. D. Rouse, M. W. Thomas, and B. T. M. Willis, J. Polym. Sci., Polym. Lett. Ed. **13**, 351 (1975).

[12] M. S. Miao, M. L. Zhang, and V. E. Van Doren, J. Chem. Phys. **115**, 11317 (2001).

[13] C. Nakafuku and T. Takemura, Jpn. J. Appl. Phys. **14**, 599 (1975).

[14] J. R. Koe, D. R. Powell, J. J. Buffy, S. Hayase, and R. West, Angew. Chem. **110**, 1514 (1998).

[15] J. Trotter, M. Akhtar, and N. Bartlett, J. Chem. Soc. A 30–33 (1966).

[16] K. Doll and M. Jansen, Angew. Chem., Int. Ed. **50**, 4627 (2011).

[17] L.-M. Wang, *Proceedings of the 25th International Conference on Microelectronics, Belgrade, Serbia and Montenegro, 14–17 May* (IEEE, New York, 2006), pp. 576–579.

[18] G. Kresse and J. Furthmuller, Phys. Rev. B **54**, 11169 (1996).

[19] J. P. Perdew, K. Burke, and M. Ernzerhof, Phys. Rev. Lett. **77**, 3865 (1996).

[20] D. C. Langreth *et al.*, Int. J. Quantum Chem. **101**, 599 (2005).

[21] S. Grimme, J. Comput. Chem. **27**, 1787 (2006).

[22] P. E. Blochl, Phys. Rev. B **50**, 17953 (1994).

[23] G. Kresse and D. Joubert, Phys. Rev. B **59**, 1758 (1999).

[24] C. S. Liu, G. Pilania, C. C. Wang, and R. Ramprasad, J. Phys. Chem. A **116**, 9347 (2012).

[25] S. Baroni, S. de Gironcoli, and A. Dal Corso, Rev. Mod. Phys. **73**, 515 (2001).

[26] M. Gajdos, K. Hummer, G. Kresse, J. Furthmuller, and F. Bechstedt, Phys. Rev. B **73**, 045112 (2006).

[27] X. Wang and D. Vanderbilt, Phys. Rev. B **75**, 115116 (2007).

[28] X. Wu, D. Vanderbilt, and D. R. Hamann, Phys. Rev. B **72**, 035105 (2005).

[29] G. Pilania and R. Ramprasad, J. Mater. Sci. **47**, 7580 (2012).

[30] T. T. Lin, X. Y. Liu, and C. B. He, J. Phys. Chem. B **116**, 1524 (2012).

[31] J. Heyd and G. E. Scuseria, J. Chem. Phys. **121**, 1187 (2004).

[32] S. Kavesh and J. M. Schultz, Polym. Sci. Part A-2, 8243 (1970).

[33] R. L. Miller and L. E. Nielsen, J. Polym. Sci. **44**, 391 (1960).

[34] B. Montanari and R. O. Jones, Chem. Phys. Lett. **272**, 347 (1997).

[35] K. J. Less and E. G. Wilson, J. Phys. C: Solid State Phys. **6**, 3110 (1973).

[36] K. Nagayama, T. Miyamae, R. Mitsumoto, H. Ishii, Y. Ouchi, and K. Seki, J. Electron Spectrosc. Relat. Phenom. **78**, 407 (1996).

[37] J. Bicerano, *Prediction of Polymer Properties*, 3rd ed. (Marcel Dekker, New York, 2002).

[38] E. N. Brothers, G. E. Scuseria, and K. N. Kudin, J. Phys. Chem. B **110**, 12860 (2006).

[39] X. Gonze and C. Lee, Phys. Rev. B **55**, 10355 (1997).

[40] X. Gonze, Phys. Rev. B **55**, 10337 (1997).

[41] P. Giannozzi and S. Baroni, J. Chem. Phys. **100**, 8537 (1994).

[42] D. Porezag and M. R. Pederson, Phys. Rev. B **54**, 7830 (1996).

[43] P. Puschnig and C. Ambrosch-Draxl, Phys. Rev. B **60**, 7891 (1999).

[44] J. A. Berger, P. L. de Boeij, and R. van Leeuwen, J. Chem. Phys. **123**, 174910 (2005).

[45] T. C. Choy, *Effective Medium Theory: Principles and Applications* (Oxford University Press, Oxford, 1999).

[46] J. A. Osborn, Phys. Rev. **67**, 351 (1945).

[47] E. C. Stoner, Phil. Mag. **36**, 803 (1945).

[48] L. D. Landau, E. M. Lifshitz, and L. P. Pitaevskii, *Electrodynamics of Continuous Media*, 2nd ed., Course of Theoretical Physics Vol. 8 (Pergamon, Oxford, 1984).

[49] M. L. T. Asaki, A. Redondo, T. A. Zawodzinski, and A. J. Taylor, J. Chem. Phys. **116**, 10377 (2002).

[50] F. W. Billmeyer, J. Appl. Phys. **28**, 1114 (1957).